Diffraction by a quarterplane of the field from a halfwave dipole

N.Chr. Albertsen

Indexing terms: Vector diffraction, Quarterplane, Halfwave dipole, Far field

Abstract: The scattered far field from a halfwave dipole illuminating a perfectly conducting quarterplane is calculated. The calculation is based on a calculation of the radial electric and magnetic field components on the far-field sphere, using uniform geometrical theory of diffraction (GTD), and subsequent conversion of the radial fields into transverse field components using two elementary Green's functions.

1 Introduction

The problem of calculating the diffraction of an electromagnetic wave around a perfectly conducting quarterplane remains a challenge in electromagnetics. More then 30 years ago Radlow published a solution to the scalar, soft quarterplane problem [1]. The paper aroused some discussion, since the order of the singularity at the vertex, according to Radlow, differed from the accepted value [2]. Extensive tests of a vertex diffraction coefficient, derived from [1], showed, however, excellent agreement with other results obtained by numerical methods, e.g. [3]. The extension of Radlow's method to the hard quarterplane is trivial, but so far no one seems to have succeeded in extending the method to the electromagnetic case. The only exact solution to that problem published to date seems to be [4], which is not amenable to an asymptotic interpretation, whereas a number of heuristic approaches have produced results that are satisfactory for practical purposes [5–7].

The present paper will consider the vector problem from an entirely new angle. Is it possible to derive a solution to the vector diffraction problem based entirely on knowledge of the solutions to the soft and hard scalar problems? The first step is to find suitable, scalar wave fields that satisfy soft or hard boundary conditions on the quarterplane. The second is to find a transformation which will produce the transverse vector components of the scattered far field from the above scalar fields.

IEE Proceedings online no. 19971151

Paper first received 27th June 1996 and in revised form 23rd January 1997

The author is with the Institute of Mathematical Modelling, Building 305, Technical University of Denmark, DK-2800, Lyngby, Denmark

2 Radial far field

Consider two scalar wave fields, u_E and u_H, defined by:

$$u_E = \mathbf{r}_A \cdot \mathbf{E}$$
$$u_H = \mathbf{r}_A \cdot \mathbf{H} \qquad (1)$$

where $\mathbf{r}_A$ is the vector from the origin to the field point. By expansion in Cartesian coordinates, it is easy to find that the two scalar fields, u_E and u_H, satisfy the Helmholtz equation in free space.

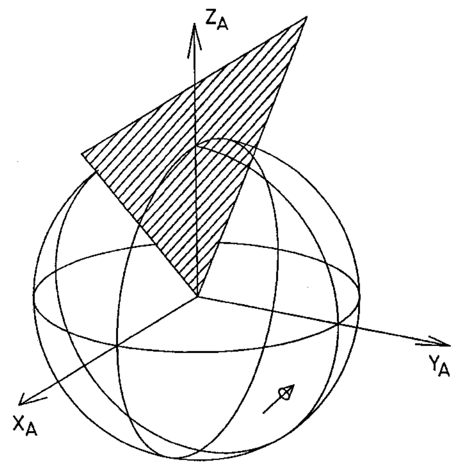

Fig. 1 *Position of quarterplane in x_A, y_A, z_A coordinate system*

It is evidently possible to calculate u_E and u_H using standard geometrical theory of diffraction (GTD) techniques for scalar fields also in the presence of scatterers, provided these can be placed in such a way that u_E and u_H satisfy suitable boundary conditions on the scatterers. For the present application we shall place the quarterplane in the $x_A - z_A$ plane as shown in Fig. 1 with the vertex at the origin and the edges forming an angle of 45° with the z_A axis. The reason behind this particular positioning will become evident in Section 3 (but, briefly, it introduces the maximum amount of symmetry when the problem is considered in spherical coordinates).

The boundary conditions for u_E and u_H on the quarterplane now become simple, homogeneous expressions:

$$u_E = 0$$
$$\frac{\partial u_H}{\partial n} = 0 \qquad (2)$$

where n is a normal to the surface. At infinity the standard Sommerfeld radiation conditions are assumed to apply.

In Fig. 1 the source is shown as a halfwave dipole, and we shall now consider how the source fields, u_E^i and u_H^i, can be derived conveniently. It can be shown that the field from a halfwave dipole can be represented exactly everywhere by the field from two point sources, $\mathbf{P}_1$ and $\mathbf{P}_2$, one at each end of the dipole, [8], p.69. The field at an arbitrary point, $\mathbf{P}_0$, can then be found as the sum of two ray fields, one from $\mathbf{P}_1$ and one from $\mathbf{P}_2$.

In Fig. 1 the centre of the dipole has been placed at $\mathbf{P}_S$, with the coordinates $(r_A, \theta_A, \phi_A) = (r_S, \theta_S, \pi/2)$, and directed along the unit vector $\mathbf{t}_s = (x_A, y_A, z_A) = (0, -\cos\theta_S, \sin\theta_S)$. The electric field vector from either of the point sources, $\mathbf{P}_1$ or $\mathbf{P}_2$, will be polarised along θ_1 or θ_2 in dipole coordinate systems centered at $\mathbf{P}_1$ and $\mathbf{P}_2$, respectively, and we notice that $\mathbf{r}_A \cdot \theta_j = C_j$, $j = 1, 2$, where C_j is constant along any (straight) ray. The amplitude variation of u_E^i along a ray is therefore entirely controlled by the transport equation in the usual manner. The same holds for u_H^i.

It is now possible to calculate the far field of u_E and u_H using standard GTD techniques. The fields from $\mathbf{P}_1$ and $\mathbf{P}_2$ are calculated separately and the rays included are, depending on the position on the far-field sphere: a direct ray, a reflected ray from the surface of the quarterplane, a diffracted ray from each of the two edges and two vertex rays. The edge diffracted rays, which include slope diffraction, are calculated using the standard UTD transition function [10] as if the edge was infinitely long. From the definition of u_E^i and u_H^i it is evident that both are zero along the ray through the vertex at the origin. Consequently, there is no diffracted ray from the vertex but, due to the variation in u_E^i and u_H^i close to the vertex, there are two slope diffraction contributions for both u_E and u_H. One of these is due to the variation of the field along θ, the other is due to the variation along ϕ, where θ and ϕ are spherical unit vectors in the quarterplane centred coordinate system used to define the uniform, scalar vertex diffraction coefficients $D_{V,S}$ and $D_{V,H}$, for the soft and hard quarterplane, respectively, details of which are given in the Appendix (Section 7). Having determined u_E and u_H on the far-field sphere, $r_A \to \infty$, it now remains to transform them into transverse $\mathbf{E}$ and $\mathbf{H}$ components: E_{θ_A}, E_{ϕ_A}, H_{θ_A}, and H_{ϕ_A}.

3 Green's function

We shall now address the problem of converting the radial field components calculated in Section 2 on the far-field sphere to transverse components. In free space this would be trivial. We could expand the radial fields in tesseral harmonics and use the expansion coefficients in a spherical expansion of the total field. The presence of the quarterplane, however, dictates the use of a different, far more complicated, set of expansion functions, e.g. [4]. A simpler approach, based on the ideas set forth in [9], will therefore be generalised to apply to the present problem.

The basic assumption for the procedure is, that on the far-field sphere, the radial field components can be expressed asymptotically as:

$$H_{r_A} = h_A(\theta_A, \phi_A)\exp(ikr_A)/r_A^2 \tag{3}$$

$$E_{r_A} = \varsigma_0 e_A(\theta_A, \phi_A)\exp(ikr_A)/r_A^2 \tag{4}$$

where ς_0 is the free space impedance and the time dependence $\exp(-i\omega t)$ is used. Furthermore, on the far-field sphere:

$$\begin{aligned} E_{\theta_A} &= \varsigma_0 H_{\phi_A} \\ E_{\phi_A} &= -\varsigma_0 H_{\theta_A} \end{aligned} \tag{5}$$

allowing us to determine all transverse field components from the functions $W_A(\theta_A, \phi_A)$ and $Z_A(\theta_A, \phi_A)$ defined through:

$$\sin\theta_A H_{\theta_A} = W_A(\theta_A, \phi_A)\exp(ikr_A)/r_A \tag{6}$$

$$\sin\theta_A H_{\phi_A} = Z_A(\theta_A, \phi_A)\exp(ikr_A)/r_A \tag{7}$$

We now insert eqns. 3, 4, 6 and 7 into Maxwell's equations and isolate the radial terms. With the transformation:

$$\psi_A = \log(\tan(\theta_A/2)) \tag{8}$$

$$\begin{aligned} w_A(\psi_A, \phi_A) &= W_A(\theta_A, \phi_A) \\ z_A(\psi_A, \phi_A) &= Z_A(\theta_A, \phi_A) \end{aligned} \tag{9}$$

the result can be expressed as the Poisson equations:

$$\frac{\partial^2 z_A}{\partial\psi_A^2} + \frac{\partial^2 z_A}{\partial\phi_A^2} = \frac{\partial f_A}{\partial\psi_A} + \frac{\partial g_A}{\partial\phi_A} \tag{10}$$

$$\frac{\partial^2 w_A}{\partial\psi_A^2} + \frac{\partial^2 w_A}{\partial\phi_A^2} = \frac{\partial g_A}{\partial\psi_A} - \frac{\partial f_A}{\partial\phi_A} \tag{11}$$

where:

$$f_A(\psi_A, \phi_A) = -ik\sin^2\theta_A e_A(\theta_A, \phi_A) \tag{12}$$

$$g_A(\psi_A, \phi_A) = -ik\sin^2\theta_A h_A(\theta_A, \phi_A) \tag{13}$$

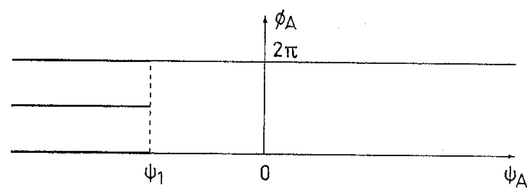

Fig.2 *Transformed coordinate system* (ψ_A, ϕ_A)

In contrast to [9] where the boundary conditions were simple, as fields in free space were being considered, the boundary conditions in ϕ_A for z_A and w_A are relatively complicated, whereas the conditions in ψ_A are that both functions must behave as rational functions at $\pm\infty$. Consider Fig. 2 which shows the mapping of the far-field sphere on the $\psi_A - \phi_A$ coordinates. Here, ψ_1 is the transform of $\theta_A = \pi/4$, so for $\psi_A > \psi_1$ we have free space conditions, i.e. simple, periodic conditions on $\phi_A = 0$ and $\phi_A = 2\pi$, while for $\psi_A < \psi_1$ the solutions to eqns. 10 and 11 must satisfy the boundary conditions on the quarterplane:

$$\begin{aligned} &z_A(\psi_A, 0) = 0 \\ &z_A(\psi_A, \pi) = 0 \\ &z_A(\psi_A, 2\pi) = 0 \quad \psi_A < \psi_1 \end{aligned} \tag{14}$$

$$\begin{aligned} &\frac{\partial w_A(\psi_A, 0)}{\partial\phi_A} = 0 \\ &\frac{\partial w_A(\psi_A, \pi)}{\partial\phi_A} = 0 \\ &\frac{\partial w_A(\psi_A, 2\pi)}{\partial\phi_A} = 0 \quad \psi_A < \psi_1 \end{aligned} \tag{15}$$

If we can find the fundamental solution to Laplace's equation with the boundary conditions of eqns. 14 and

15, we can use Green's method to express the solutions to eqns. 10 and 11 in integral form. The topology of the problem suggests that the solution of coupled Wiener-Hopf equations may be required, since the combination of boundary conditions seems unsuitable for the application of conformal mapping. As will be shown it is possible, though, to apply certain transformations which change the problem into one that may be solved by conformal mapping.

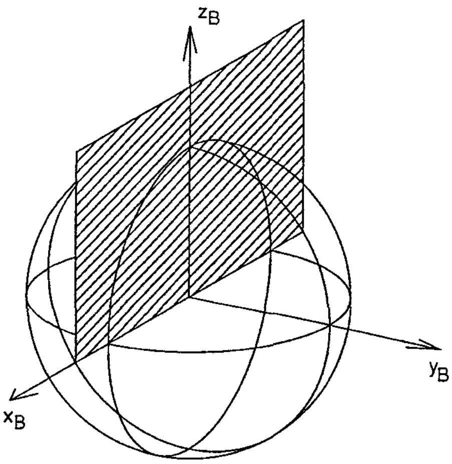

Fig. 3 *Equivalent halfplane in x_B, y_B, z_B coordinates*

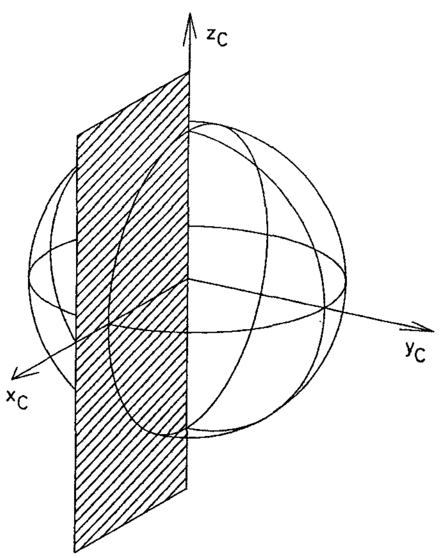

Fig. 4 *Equivalent halfplane in x_C, y_C, z_C coordinates*

We first observe that the value of ψ_1 enters into the problem in a trivial manner. If we introduce the transformation:

$$\begin{aligned} \psi_B &= \psi_A - \psi_1 \\ \theta_B &= 2\arctan(\exp(\psi_B)) \\ \phi_B &= \phi_A \end{aligned} \tag{16}$$

we obtain a problem for $z_B(\psi_B, \phi_B)$ and $w_B(\psi_B, \phi_B)$ described by eqns. 10–15, replacing the subscript A with B and replacing ψ_1 with zero in eqns. 14 and 15. Apparently this problem is no simpler than the original one, but if we consider the three-dimensional geometry, which maps onto these boundary conditions on the far-field sphere, we find Fig. 3, i.e. a mapping of a halfplane. Obviously, Fig. 3 is only valid on the far-field sphere, so it has no meaning to show the image of the source. Fig. 3 strongly suggests yet another transformation from the (r_B, θ_B, ϕ_B) coordinate system in Fig. 3 to the (r_C, θ_C, ϕ_C) coordinate system in Fig. 4, where the halfplane has been turned through 90°. We can express the connection between the B and C coordinates through simple trigonometric relations.

Again we introduce a transformation in θ as:

$$\psi_C = \log(\tan(\theta_C/2)) \tag{17}$$

and let:

$$\begin{aligned} e_C(\theta_C, \phi_C) &= e_B(\theta_B, \phi_B) \\ &= \frac{\sin^2\theta_A}{\sin^2\theta_B} e_A(\theta_A, \phi_A) \end{aligned} \tag{18}$$

$$\begin{aligned} h_C(\theta_C, \phi_C) &= h_B(\theta_B, \phi_B) \\ &= \frac{\sin^2\theta_A}{\sin^2\theta_B} h_A(\theta_A, \phi_A) \end{aligned} \tag{19}$$

where the right hand sides are obtained from eqns. 12 and 13.

Introducing:

$$f_C(\psi_C, \phi_C) = -ik\sin^2\theta_C e_C(\theta_C, \phi_C) \tag{20}$$

$$g_C(\psi_C, \phi_C) = -ik\sin^2\theta_C h_C(\theta_C, \phi_C) \tag{21}$$

we can then formulate a problem for $z_C(\psi_C, \phi_C)$ and $w_C(\psi_C, \phi_C)$ which is similar to eqns. 10 and 11, except for the subscripts which are changed from A to C. The advantage gained lies in the boundary conditions, which can now be expressed as:

$$\begin{aligned} z_C(\psi_C, 0) &= 0 \\ z_C(\psi_C, 2\pi) &= 0 \end{aligned} \tag{22}$$

$$\begin{aligned} \frac{\partial w_C(\psi_C, 0)}{\partial\phi_C} &= 0 \\ \frac{\partial w_C(\psi_C, 2\pi)}{\partial\phi_C} &= 0 \end{aligned} \tag{23}$$

for all values of ψ_C. It is now elementary to find the fundamental solution to Laplace's equation by conformal mapping. The result is:

$$G_D(\psi_C, \phi_C) = \frac{1}{4\pi}\log\frac{G_1}{G_2} \tag{24}$$

$$G_N(\psi_C, \phi_C) = \frac{1}{4\pi}\{\log 4 + \psi_C + \psi_C^0 + \log(G_1 G_2)\} \tag{25}$$

for the Dirichlet and Neumann condition, respectively, where:

$$G_1 = \cosh((\psi_C - \psi_C^0)/2) - \cos((\phi_C - \phi_C^0)/2) \tag{26}$$

$$G_2 = \cosh((\psi_C - \psi_C^0)/2) - \cos((\phi_C + \phi_C^0)/2) \tag{27}$$

The solution to $z_C(\psi_C, \phi_C)$ and $w_C(\psi_C, \phi_C)$ can then be expressed as:

$$z_C(\psi_C, \phi_C) = \int_{-\infty}^{\infty} d\psi_C^0 \int_0^{2\pi} \left\{ \frac{\partial f_C(\psi_C^0, \phi_C^0)}{\partial\psi_C^0} + \frac{\partial g_C(\psi_C^0, \phi_C^0)}{\partial\phi_C^0} \right\} G_D d\phi_C^0 \tag{28}$$

$$w_C(\psi_C,\phi_C) = \int_{-\infty}^{\infty} d\psi_C^0 \int_0^{2\pi} \left\{ \frac{\partial g_C(\psi_C^0,\phi_C^0)}{\partial \psi_C^0} - \frac{\partial f_C(\psi_C^0,\phi_C^0)}{\partial \phi_C^0} \right\} G_N d\phi_C^0 \tag{29}$$

Since f_C and g_C are only known numerically, whereas the analytical form of G_D and G_N are known, it is preferable to perform a number of partial integrations. As it can be shown [9] that the endpoint contributions vanish, we find:

$$z_C(\psi_C,\phi_C) = -\int_{-\infty}^{\infty} d\psi_C^0 \int_0^{2\pi} \left\{ f_C \frac{\partial G_D}{\partial \psi_C^0} + g_C \frac{\partial G_D}{\partial \phi_C^0} \right\} d\phi_C^0 \tag{30}$$

$$w_C(\psi_C,\phi_C) = -\int_{-\infty}^{\infty} d\psi_C^0 \int_0^{2\pi} \left\{ g_C \frac{\partial G_N}{\partial \psi_C^0} - f_C \frac{\partial G_N}{\partial \phi_C^0} \right\} d\phi_C^0 \tag{31}$$

Using eqns. 6–9, replacing subscript A with C, we can, from eqns. 30 and 31, determine H_{θ_C} and H_{ϕ_C}. By some straightforward calculations we can then find the field components along $\underline{\theta}_B(\theta_B, \phi_B)$ and $\underline{\phi}_B(\theta_B, \phi_B)$: $H_{\theta_B}(\theta_B, \phi_B)$ and $H_{\phi_B}(\theta_B, \phi_B)$. Turning again to eqns. 6–9, replacing the subscript A with B this time, we can then calculate $z_B(\psi_B, \phi_B)$ and $w_B(\psi_B, \phi_B)$ from which, by virtue of eqn. 16, we can find $z_A(\psi_A, \phi_A)$ and $w_A(\psi_A, \phi_A)$ and, hence, through a final application of eqns. 5–9, the solution to our problem, $H_{\theta_A}(\theta_A, \phi_A)$, $H_{\phi_A}(\theta_A, \phi_A)$, $E_{\theta_A}(\theta_A, \phi_A)$ and $E_{\phi_A}(\theta_A, \phi_A)$.

To obtain H_{θ_C} and H_{ϕ_C} from eqns. 30 and 31, $z_C(\psi_C, \phi_C)$ and $w_C(\psi_C, \phi_C)$ must be divided by $\sin\theta_C$. It is therefore essential that the integrals in eqns. 30 and 31 tend to zero for $|\psi_C| \to \infty$. Due to the structure of G_D it is clear that eqn. 30 fulfils this requirement. It is less obvious that, also eqn. 31 has the required property. Since G_N contains a linear term in ψ_C^0, its partial derivative with respect to ψ_C^0 tends to a constant for $|\psi_C| \to \infty$. The first term in the integrand in eqn. 31 must therefore be considered separately, whereas the second presents no problems. It is thus necessary to require that the integral of g_C over the entire region is zero. Changing the integration coordinates to (θ_C^0, ϕ_C^0) it is a simple matter to verify that we can restate the condition to be that the integral of $h_C(\theta_C, \phi_C)$ over the far-field sphere must be zero. Since this integral is invariant with respect to the transformations introduced, we may as well require the integral of $h_A(\theta_A, \phi_A)$ to have this property. To prove that this is true, we introduce a region Υ with boundary $\partial\Upsilon$ consisting of:

(1) Two infinitesimal spheres around the two point sources ($\partial\Upsilon_1$);

(2) Two quarterplanes displaced infinitesimally to either side of the real quarterplane ($\partial\Upsilon_2$);

(3) The far-field sphere, cut along the intersection with the real quaterplane ($\partial\Upsilon_3$).

The interior of Υ is a free-space region where $\nabla\cdot\mathbf{H} = 0$. By Gauss' theorem the total outward flux of $\mathbf{H}$ through $\partial\Upsilon$ must therefore be zero. Since the sources were carefully chosen to have no radial field components, the flux through $\partial\Upsilon_1$ is zero and, due to the boundary conditions for $\mathbf{H}$ on the quarterplane, there is no flux through $\partial\Upsilon_2$ either. It follows thus that the flux though $\partial\Upsilon_3$ is zero as required.

4 Numerical results

To test the method, the configuration in Fig. 1 was used with $r_S = 8/k$ and $\theta_S = 135°$. The choice of r_S is a compromise between making r_S large to make the incident field less characteristic of the specific source used, and making r_S small to reduce the oscillatory behaviour of the integrands in eqns. 30 and 31 and thus to avoid excessive computing times. The choice of θ_S avoids irrelevant complications due to multiple edge diffractions.

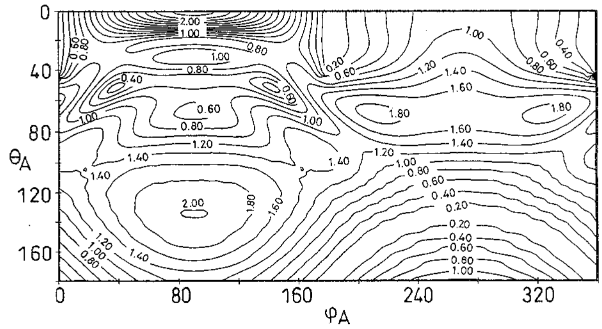

Fig. 5 *Diffracted $E_{\theta A}$ field around quarterplane*

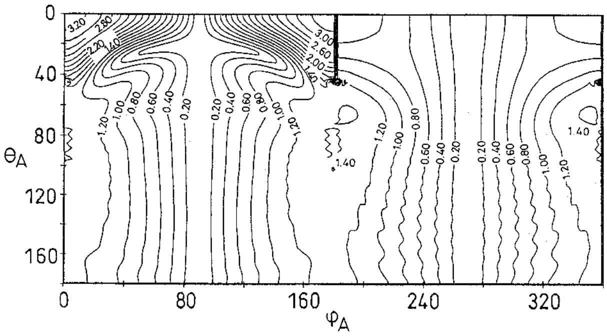

Fig. 6 *Diffracted $E_{\phi A}$ field around quarterplane*

The results of the calculations are shown in Figs. 5 and 6 as linear amplitude contour plots with equispaced contours between zero and the maximum amplitude. The traces of the quarterplane are clearly visible at $\phi_A = 0°$, 180° and 360° between $\theta_A = 0°$ and 45°. To get an indication of the influence of the vertex contribution, another calculation was made based entirely on [10]. The source was still represented by two point sources, but now the θ components of the source rays were used to calculate the reflected and edge diffracted rays. The result of this calculation showed an excellent general agreement with Figs. 5 and 6 except for the following differences: in the region of the traces of the Keller cones for the vertex there are significant differences, since the field of the edge diffracted rays is discontinuous here, and the ripples on the contour lines in Figs. 5 and 6 for large values of θ_A are absent.

5 Conclusions

The paper presents a method by which the vector diffraction problem for the quarterplane can be solved on the basis of the solutions to the two scalar diffraction problems for the quarterplane, namely the soft boundary and the hard boundary cases. The method could in principle be extended to other geometries for which the scalar, but not the vector, solutions are known. However, since the scatterer must transform into a simple boundary shape in (ψ, ϕ) coordinates with homogeneous boundary conditions for the $w(\psi, \phi)$ and $z(\psi, \phi)$ functions, it seems that only plane, angular sectors (of which the quarterplane is a special case) and circular cones are candidates, restricting the generality of the method considerably. Due to the time consuming calculations involved in eqns. 30 and 31, the usefulness of the solution presented will mostly lie in its ability to generate highly accurate benchmark results against which other, heuristic, but faster, methods can be tested.

6 References

1 RADLOW, J.: 'Note on the diffraction at a corner', *Arch. Rational Mech. Anal.*, 1965, **19**, pp. 62–70
2 KRAUS, L., and LEVINE, L.M.: 'Diffraction by an elliptic cone', *Comm. on Pure and Appl. Math.*, 1961, **14**, pp. 49–68
3 TEW, M., and MITTRA, R.: 'On a spectral domain approach for testing Albertsen's corner diffraction coefficient', *Radio Sci.*, 1980, **15**, pp. 587–594
4 SATTERWHITE, R.S.: 'Diffraction by a quarter plane, the exact solution and some numerical results', *IEEE Trans.*, 1974, **AP-22**, pp. 500–503
5 HANSEN, T.B.: 'Corner diffraction coefficients for the quarter plane', *IEEE Trans.*, 1991, **AP-39**, pp. 976–984
6 IVRISSIMTZIS, L.P., and MARHEFKA, R.J.: 'Edge wave vertex and edge diffraction', *Radio Sci.*, 1989, **24**, pp. 771–784
7 MACI, S., and TIBERIO, R.: 'Diffraction of a plane angular sector', *J. Electromagn. Waves Appl.*, 1994, **8**, pp. 1247–1276
8 BACH, H., PONTOPPIDAN, K., and SOLYMAR, L.: 'High frequency radiation pattern prediction for satellite antennas'. Final report R121, ESTEC contract 1821/72, Electromagnetics Institute, Technical University of Denmark, Lyngby, 1973
9 ALBERTSEN, N.C.: 'Green's function for determining transverse E.M. field components from the radial components', *Electron. Lett.*, 1976, **12**, pp. 542–544
10 KOUYOUMJIAN, R.G., and PATHAK, P.H.: 'A uniform geometrical theory of diffraction for an edge in a perfectly conducting surface', *Proc. IEEE*, 1974, **62**, pp. 1448–1461
11 ALBERTSEN, N.C., BACH, H., BALLING, P., SØRENSEN, O., and PONTOPPIDAN, K.: 'Radiation pattern prediction for high frequency antennas'. Final report R183, ESTEC contract 2866/76, Electromagnetics Institute, Technical University of Denmark, Lyngby, 1977
12 NIELSEN, N.: 'Der Eulersche Dilogarithmus und seine Verallgemeinerungen', *Nova Acta, Abh. der Kaiserl. Leop.-Carol. Deutschen Akademie der Naturforscher, Halle*, 1909, **90**, pp. 125–211

7 Appendix: Scalar vertex diffraction coefficients

Following Radlow [1] we shall derive the uniform, vertex diffraction coefficients for the quarterplane in a coordinate system, where the quarterplane is placed with its edges along the positive x and y axes. Radlow considers a soft quarterplane illuminated by a plane wave with unit amplitude incident from the direction $(\theta, \phi) = (\theta_0, \phi_0)$, and derives an expression for the total, scattered field which, with some change in notation, is:

$$u(x,y,z) = \frac{1}{(2\pi)^2} \int_{-\infty}^{\infty} d\mu \int_{-\infty}^{\infty} M^{++}(\mu, -k_2) M^{++}(-k_1, \lambda) \times M^{++}(-k_1, -k_2) M^{++}(\mu, \lambda) \times \frac{\exp(i(\pm\gamma z - \mu x - \lambda y))}{\gamma(\mu - k_1)(\lambda - k_2)} d\lambda, \quad z \gtrless 0 \tag{32}$$

where $k_1 = k \sin\theta_0 \cos\phi_0$, $k_2 = k \sin\theta_0 \sin\phi_0$, $\gamma = \sqrt{(k^2 - \mu^2 - \lambda^2)}$ and $M^{++}(\mu, \lambda)$ is derived from two consecutive Wiener-Hopf factorisations of γ. The first of these, i.e. in λ, is elementary, the second, in μ, then becomes:

$$\sqrt{\sqrt{k^2 - \mu^2} + \lambda} = M^{++}(\mu, \lambda) M^{-+}(\mu, \lambda) \tag{33}$$

which can be solved by standard use of Cauchy's theorem to yield:

$$M^{++}(\mu, \lambda) = \sqrt[4]{\frac{k}{2}} \sqrt{1 - d_1} \exp\tau \tag{34}$$

where:

$$\begin{aligned}\tau = -\frac{1}{4\pi i} \Big\{ & Dilog(1 - d_1) - Dilog(1 + d_1) \\ & + Dilog(1 - d_2) - Dilog(1 + d_2) \\ & - i\pi Log(-\zeta_2) - \Big(Log(-id_1) - i\frac{\pi}{2}\Big) Log(1+d_1) \\ & + \Big(Log(-id_1) + i\frac{\pi}{2}\Big) Log(1 - d_1) \\ & + \Big(Log(id_2) - i\frac{\pi}{2}\Big) Log(1 - d_2) \\ & - \Big(Log(id_2) + i\frac{\pi}{2}\Big) Log(1 + d_2) \Big\}\end{aligned} \tag{35}$$

Here Log is the principal branch of log, and the Dilog function [12] is defined by:

$$Dilog(z) = -\int_1^z \frac{Log\zeta}{\zeta - 1} d\zeta \tag{36}$$

and:

$$\begin{aligned} d_1 &= \zeta_1 \kappa_1 \\ d_2 &= \zeta_1 \kappa_2 \end{aligned} \tag{37}$$

$$\left.\begin{matrix}\zeta_1 \\ \zeta_2\end{matrix}\right\} = -\frac{1}{k}\left(\lambda \mp i\sqrt{k^2 - \lambda^2}\right) \tag{38}$$

$$\left.\begin{matrix}\kappa_1 \\ \kappa_2\end{matrix}\right\} = \frac{1}{k}\left(i\mu \pm \sqrt{k^2 - \mu^2}\right) \tag{39}$$

To extract the diffraction coefficient for the vertex, we now perform two consecutive saddle point evaluations around the saddle points of the exponential in eqn. 32 using the method of UTD [10]. If we let u_{ss} denote the saddle point contribution, we find:

$$u_{ss} = \left(\frac{\exp(i\pi/4)}{\sqrt{8\pi k}}\right)^2 \frac{\exp(ikr)}{r} D_{V,S} \tag{40}$$

$$\begin{aligned} D_{V,S} &= -\frac{4}{k} \frac{M(\theta_0, \phi_0, \theta, \phi)}{(\sin\theta\cos\phi + \sin\theta_0\cos\phi_0)(\sin\theta\sin\phi + \sin\theta_0\sin\phi_0)} \\ &\quad \times \bar{F}(kr(1 + \cos(\beta_x + \beta_{x0})))\bar{F}(kr(1 + \cos(\beta_y + \beta_{y0}))) \end{aligned} \tag{41}$$

where (r, θ, ϕ) is the observation point in spherical coordinates, $F()$ is the UTD transition function (conjugated since [10] uses the time dependence $\exp(j\omega t)$) and:

$$\begin{aligned} M(\theta_0, \phi_0, \theta, \phi) &= M^{++}(-k\sin\theta\cos\phi, -k\sin\theta\sin\phi) \\ &\quad \times M^{++}(-k\sin\theta\cos\phi, -k\sin\theta_0\sin\phi_0) \\ &\quad \times M^{++}(-k\sin\theta_0\cos\phi_0, -k\sin\theta\sin\phi) \\ &\quad \times M^{++}(-k\sin\theta_0\cos\phi_0, -k\sin\theta_0\sin\phi_0) \end{aligned} \tag{42}$$

The angles denoted β refer to the angles between the incident or the diffracted ray at the vertex and the edges of the quarterplane, specifically:

$$\begin{aligned} \cos\beta_x &= \mathbf{r} \cdot \mathbf{x} \\ \cos\beta_{x0} &= -\mathbf{r}^i \cdot \mathbf{x} \end{aligned} \tag{43}$$

$$\cos\beta_y = \mathbf{r}\cdot\mathbf{y}$$
$$\cos\beta_{y0} = -\mathbf{r}^i\cdot\mathbf{y} \tag{44}$$

where $\mathbf{r}^i$ is a unit vector along the incident ray and $\mathbf{r}$ a unit vector along the diffracted ray.

It is trivial to copy Radlow's procedure for a hard quarterplane, and the resultant diffraction coefficient becomes:

$$D_{V,H} = \frac{4k\cos\theta\cos\theta_0}{M(\theta_0,\phi_0,\theta,\phi)} \times \frac{\bar{F}(kr(1+\cos(\beta_x+\beta_{x0})))\bar{F}(kr(1+\cos(\beta_y+\beta_{y0})))}{(\sin\theta\cos\phi+\sin\theta_0\cos\phi_0)(\sin\theta\sin\phi+\sin\theta_0\sin\phi_0)} \tag{45}$$

The diffraction coefficients $D_{V,E}$ and $D_{V,H}$ are derived for an incident plane wave and an observation point at a finite distance, r, but, due to reciprocity, they may also be used to calculate the far field for a source point at a finite distance.

To derive the slope diffraction coefficients for the field from a point source in $\mathbf{P}_0$, we first define two orthogonal axes through the vertex along the unit vectors $\mathbf{c}_1$ and $\mathbf{c}_2$, both of which are also orthogonal to the incident ray from $\mathbf{P}_0$. Furthermore, let $\mathbf{c}_1$ lie in a plane through the z axis and therefore be parallel to θ_0 in $\mathbf{P}_0$, while $\mathbf{c}_2$ is parallel to ϕ_0. Following [11] we represent the slope field at the vertex along $\mathbf{c}_1$ by that from a doublet of sources displaced $\pm\Delta$ around $\mathbf{P}_0$ along θ_0. The diffracted ray from each member of the doublet is calculated and summed, and finally $\Delta \to 0$ leads to a slope contribution:

$$u_{slope,\theta} = \frac{\partial u^i}{\partial c_1}\left(-\frac{1}{ik}\frac{\partial D_V}{\partial\theta_0}\right) \tag{46}$$

where D_v may be either $D_{V,S}$ or $D_{V,H}$ and u^i is the field from the original source in $\mathbf{P}_0$ at the vertex. Repeating the procedure along $\mathbf{c}_2$ instead provides the second contribution:

$$u_{slope,\phi} = \frac{\partial u^i}{\partial c_2}\left(-\frac{1}{ik\sin\theta_0}\frac{\partial D_V}{\partial\phi_0}\right) \tag{47}$$